

Optical Engineering

SPIDigitalLibrary.org/oe

Plasma enhancement of femtosecond laser-induced electromagnetic pulses at metal and dielectric surfaces

Sanjay Varma
Jane Spicer
Benjamin Brawley
Joseph Miragliotta

Plasma enhancement of femtosecond laser-induced electromagnetic pulses at metal and dielectric surfaces

Sanjay Varma,* Jane Spicer, Benjamin Brawley, and Joseph Miragliotta

Johns Hopkins University Applied Physics Laboratory, Laurel, Maryland 20723

Abstract. In a previous report, we have shown that the long wavelength, electromagnetic-pulsed (EMP) energy generated by ultrashort (38 fs) laser pulse ablation of a metal target is enhanced by an order of magnitude due to a preplasma generated by a different, 14-ns-long laser pulse. Here, we further investigate this EMP enhancement effect in a 2- to 16-GHz microwave region with different target materials and laser parameters. Specifically, we show a greater than two orders of magnitude enhancement to the EMP energy when the nanosecond and ultrashort laser pulses are coincident on a glass target, and greater than one order of magnitude enhancement when the pulses are coincident on a copper target. © The Authors. Published by SPIE under a Creative Commons Attribution 3.0 Unported License. Distribution or reproduction of this work in whole or in part requires full attribution of the original publication, including its DOI. [DOI: 10.1117/1.OE.53.5.051515]

Keywords: lasers; materials; laser-induced damage; ultrafast; femtosecond; plasma.

Paper 131303SS received Aug. 26, 2013; revised manuscript received Feb. 26, 2014; accepted for publication Mar. 17, 2014; published online Apr. 22, 2014.

1 Introduction

Kerr-lens mode locking and chirped pulse amplification have made high energy, ultrashort infrared laser pulses available to researchers around the world. As a result of their intense peak powers, generation of electromagnetic radiation at many different frequencies is possible through the nonlinear interaction of these laser pulses with solid, liquid, and gas phase materials. For example, ultrashort pulses may be frequency up-converted into UV, soft and hard x-ray sources through harmonic generation.^{1,2} Similarly, intense ultrashort pulses incident on solid targets can ionize inner-shell electrons, resulting in $K\alpha$ fluorescence line radiation.³ In addition to short wavelength generation phenomena, ultrashort pulses can also be frequency down-converted to mid-infrared wavelengths through the nonlinear processes of optical parametric amplification,⁴ difference frequency generation,⁵ and optical rectification.⁶ Broadband terahertz (THz) pulses are emitted through optical rectification in nonlinear crystals,⁷ from subpicosecond-irradiated photoconductive switches,⁸ and from femtosecond pulses propagating in atmosphere while generating plasma filaments.⁹ High-energy broadband THz radiation has also been observed when an ultrashort pulse is mixed with its second harmonic to generate plasma in air.¹⁰ As a result of the short duration of the femtosecond pulse, the broadband long wavelength radiation typically extends from the radio frequency (RF) through the THz region of the spectrum, and is referred to as an electromagnetic pulse (EMP).

EMP in the RF spectrum that arose from target irradiation and ablation with subnanosecond pulses was observed as early as 1978.¹¹ In the TITAN, (Livermore, California) petawatt-scale laser facility at Lawrence Livermore National Laboratory, investigators observed that a 2 ps, hundreds of joules laser pulse incident on a silver foil generated EMP

with amplitude ranging from 10 to 100 V/m.¹² In the aforementioned case, EMP radiation was attributed to the heating of electrons at the laser focus and subsequent acceleration of those electrons away from the target surface. However, for ultrashort laser pulses of moderate intensity (10^{13} to 10^{15} W/cm²) incident on gas, solid dielectric, and metal targets, the dominant mechanism for EMP formation is understood to be the laser-induced ponderomotive electromagnetic potential driving free electrons away from the laser focus in the radial and axial directions. Sprangle et al.¹³ simulate and discuss in detail the theory behind this proposed mechanism.

Aspiotis et al.¹⁴ measured the spectrum and amplitude of EMP due to an ultrashort laser pulse focused 5 cm onto copper and dielectric targets at 10^{17} -W/cm² intensity between 1 and 40 GHz. We have previously measured magnitude, directionality, and polarization of EMP (10 GHz) due to a 40 fs, 800-nm pulse focused in atmosphere at 25-cm range onto several metals, semiconductors, and dielectric targets.¹⁵

In this current investigation, we further examine the enhancement of ultrashort laser-induced EMP observed in Ref. 16. In that work, we showed evidence that nanosecond laser pulse-induced plasma on a copper surface prior to the arrival of a second, ultrashort laser pulse (38-fs FWHM) enhanced the EMP emission in the 2 to 18-GHz range by nearly an order of magnitude relative to the EMP from an individual femtosecond laser source.¹⁶ The nanosecond laser pulse was considered the pump, and the 38-fs pulse was considered the probe. As these experiments were performed in air, we also showed that nonlinear self-focusing and filamentation of the ultrashort laser pulse in atmosphere resulted in roll-off of EMP energy as a function of increasing laser pulse energy. In the current publication, we have investigated the nanosecond laser plasma-enhanced EMP with finer pump/probe time resolution. We also demonstrate, for the first time, plasma-enhanced EMP on a transparent glass dielectric surface.

*Address all correspondence to: Sanjay Varma, E-mail: sanjay.varma@jhuapl.edu

2 Experimental Setup

The ultrashort laser pulse used for the experiment was 38-fs FWHM in duration and had 42-mJ energy and an 800-nm center wavelength (Mantis oscillator and Hydra regenerative and multipass amplifiers, Coherent, Inc., Santa Clara, California). We measured the pulse length before each experiment with a single-shot autocorrelator. In these current experiments, the 38-fs laser pulse had 20% higher energy than our previous pump/probe experiment.¹⁶ The 14 ns FWHM, 1064-nm wavelength pulse was generated by a flashlamp-pumped Nd:YAG laser with 390-mJ energy (Inlite III, Continuum, San Jose, California). The 14-ns laser pulse had 90% higher energy than in the previous experiment.

Both pulses were focused onto the target with the same 25-cm focal length lens with $f/\# = 17$ for the 38-fs pulse and $f/\# = 40$ for the 14-ns pulse. All laser-target measurements were performed at room temperature and atmospheric pressure. The 14-ns pulse is focused to a 0.3-mm diameter, with a fluence of 760 J/cm^2 , and a peak intensity of 20 GW/cm^2 . The peak fluence of the 38-fs pulse was $\sim 20 \text{ J/cm}^2$. As discussed previously,¹⁶ the peak fluence of the 38-fs pulse was limited by defocusing due to ionization in atmosphere. This, along with the nonlinear self-focusing that causes optical/plasma filamentation,¹⁷ is one of the consequences of focusing energetic, ultrashort pulses in atmosphere. Prior to reaching the target, nonlinear self-focusing caused hot spots in the 38-fs laser pulse to develop and eventually ionize trails of N_2 and O_2 in atmosphere, creating a number of laser plasma filaments that were incident on the sample target. Using a beam profile image and integrating along a 38-fs FWHM laser pulse duration at the target (roughly Gaussian temporal shape), we estimate the peak ultrashort laser intensity to be $\sim 5 \times 10^{14} \text{ W/cm}^2$. The beam profile of the filamenting ultrashort laser pulse is difficult to measure near the target, but we assume that the hard focal geometry ensures fast enough divergence after filamentation that linear beam imaging will give a sufficiently accurate beam profile. The ultrashort pulse spatial FWHM was 0.4 mm, which slightly overfills the nanosecond laser focal spot. We additionally note that because of self-phase modulation and dispersion in atmosphere, it is likely that the ultrashort laser pulse is no longer spatially or temporally Gaussian at the target surface.

There is some evidence to believe that the overall intensity of the femtosecond laser pulse at the target is likely lower than calculated. Mlejnek et al.¹⁸ simulated atmospheric propagation of filamenting optical pulses and predicted, as others subsequently have,^{19,20} that laser pulses with power higher than the critical power for self-focusing experience both self-steepening and spatio-temporal breakup. This leads to higher peak intensity but overall lower intensity. Recent advances in techniques for modeling and simulation of high-intensity light pulses have been reviewed.²¹ The optical intensity deliverable by ultrashort pulses in solid, liquid, and gaseous media is limited by self-focusing and filamentation in the atmosphere, well as energy loss from plasma generation.

The nanosecond and femtosecond laser pulses were synchronized with 0.5-ns jitter through the use of a Stanford Research DG535 digital delay generator. A fast photodiode was used to monitor the relative delay between laser pulses and served as a trigger signal to the RF

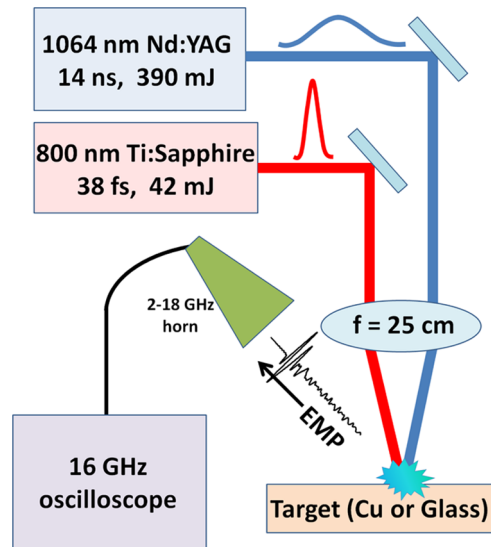


Fig. 1 Experimental setup for broadband detection of ultrashort pulse-induced EMP.

measurement setup. The entire experiment takes place at atmospheric temperature and pressure.

We measured the EMP emission with a broadband 2 to 18-GHz RF horn (Condor Systems, McLean, Virginia, AS-48461) whose input is placed 45 cm from the target at an angle of 27 deg from normal incidence in the horizontal direction. The horizontally polarized output of the horn was directly fed without amplification into a 16-GHz analog bandwidth oscilloscope (Agilent Technologies, Santa Clara, California Infiniium, DSO-X 91694A). Figure 1 shows a diagram of the broadband microwave detection setup.

3 Results and Discussion

Figure 2 shows the broadband EMP emission captured by the RF horn when the 42 mJ, 38-fs pulse was focused onto a transparent borosilicate glass target with 1-mm thickness. The oscilloscope signal was averaged over 100 shots. The black trace shows the EMP signal when the femtosecond pulse is incident on the glass target while the red trace shows the EMP response from the femtosecond pulse is incident on nanosecond laser pulse-induced plasma at the target. The peak of the femtosecond pulse leads the peak of the nanosecond pulse by 6 ns. This pump/probe delay was optimized for maximum enhanced EMP energy within

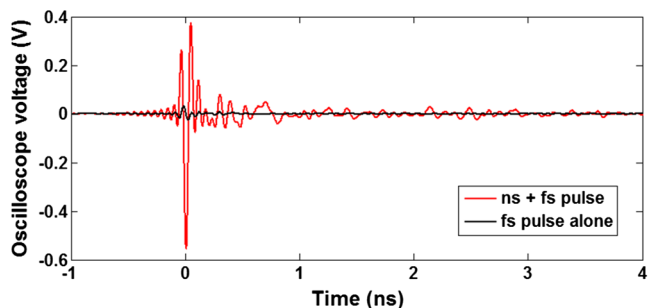


Fig. 2 2- to 16-GHz EMP generated by a 42 mJ, 38-fs pulse incident on borosilicate glass. (Black) femtosecond pulse alone and (red) femtosecond pulse incident on nanosecond pulse-generated plasma.

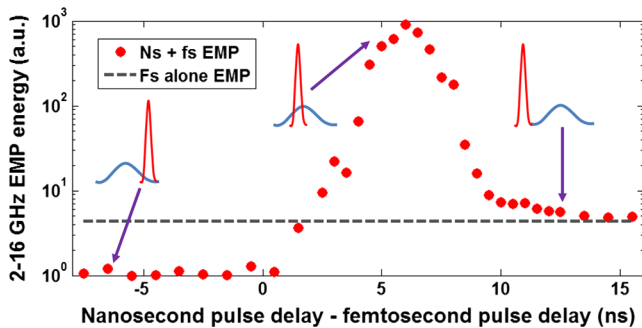


Fig. 3 2 to 16-GHz EMP energy versus pump (nanosecond laser)/probe (femtosecond laser) delay when the laser pulses are incident on a borosilicate glass target. The dashed line indicates the EMP energy generated by the probe pulse alone.

the 2 to 16-GHz range. The maximum peak-to-peak voltage swing is 0.93 V for the enhanced EMP and only 57 mV for the EMP generated by femtosecond pulse alone.

Although the largest measured EMP oscillations occur within the first 300 ps of irradiation, there was significant signal over the subsequent 3 to 4 ns. The charged particles in the plasma may only be ponderomotively driven over the duration of the laser pulse, which is <100 fs, whereas hydrodynamic expansion of the plasma happens over a nanosecond time scale. Extended ringing in the EMP signal indicates thermally driven as well as ponderomotively driven electrons.

In Fig. 3, we show the pump/probe delay dependence of the 2 to 16-GHz EMP energy emission from the borosilicate glass target. The inset figures illustrate the relative delay between the pump and probe pulses (early, coincident, and late) for three specific data points. The delay between pump and probe pulses was scanned in 0.5-ns steps. Since the timing jitter between pulses was 0.5 ns, we were not able to resolve dynamics that may occur for smaller pump/probe delay steps. The EMP energy is proportional to the time integral $\int_{-\infty}^{\infty} V^2 dt$.

The greatest EMP enhancement occurred when the peak of the femtosecond pulse precedes the peak of the nanosecond laser pulse by 6 ns. We note that because the nanosecond laser pulse has 14-ns FWHM duration, at 6 ns pump/probe delay, a significant fraction of the nanosecond pulse has entered the target prior to the femtosecond pulse. The onset of the effect of the nanosecond pulse on the femtosecond pulse occurs when the femtosecond pulse precedes the nanosecond pulse by 13 ns. This demonstrates that the plasma generated by the nanosecond pulse begins to form at least 13 ns before the nanosecond laser reaches its full intensity. When the nanosecond pulse leads the femtosecond pulse, the femtosecond-generated EMP is significantly quenched, indicating that after the peak of the nanosecond pulse, the plasma density is high enough and the plasma is large enough to refract or reflect much of the femtosecond pulse. For a wavelength of 800 nm, the critical plasma density $n_{cr} = 1.7 \times 10^{21} \text{ cm}^{-3}$.

We also measured the nanosecond plasma-enhanced EMP generated on a $5 \times 5 \text{ cm}^2$ copper target with 1-mm thickness. Figure 4 demonstrates the pump/probe delay dependence of the 2 to 16-GHz EMP energy emission. Some of the features of this relationship are similar to those observed with the glass target. Specifically, the EMP enhancement occurs at

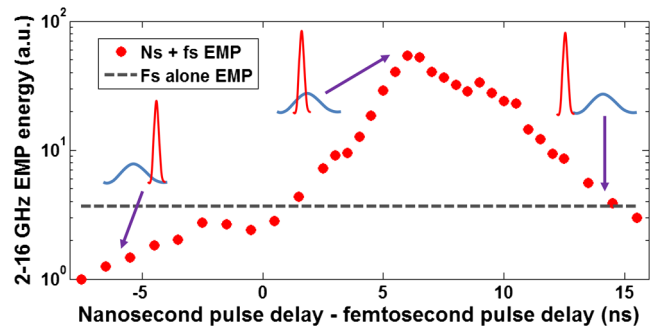


Fig. 4 2 to 16-GHz EMP energy versus pump (nanosecond laser)/probe (femtosecond laser) delay when the laser pulses are incident on a copper target. The dashed line indicates the EMP energy generated by the probe pulse alone.

6-ns pump/probe delay and is quenched as long as the peak of the femtosecond probe lags the peak of the nanosecond pump.

There are, however, some notable differences between the experiments performed on the copper and glass targets. Most obvious is that, with the copper target, the enhancement effect of the nanosecond pulse-generated plasma occurs even when the nanosecond pulse follows the femtosecond pulse by more than 13 ns. This indicates that the nanosecond pulse induces a significant plasma density on the copper surface earlier in time than on the glass surface. Copper is a metal and has free conduction band electrons (no band gap). The nanosecond pulse, even at early times when the intensity is low, may be able to generate a surface plasma that more efficiently absorbs the femtosecond laser pulse by overcoming only the work function of copper, which is 4.5 to 4.9 eV.²² The total average ionization energy of glass, on the other hand, is 11.8 eV (silicon and oxygen have ionization potentials of 8.15 and 13.62 eV, respectively) even though the band gap of borosilicate glass is only 4 eV.²³ The fact that the copper target is more easily ionized also may explain the observation that the copper EMP enhancement is roughly an order of magnitude less than the glass EMP enhancement. Although the peak-to-peak voltages of the enhanced EMP are nearly identical for copper and glass, the femtosecond pulse alone makes significantly more EMP on the copper target than it does on glass.

The explanation of the enhancement of EMP energy at 6-ns pump/probe delay is difficult without modeling or experimentally diagnosing the plasma density. We hypothesize that the enhancement is due to an outer layer of preformed plasma that is near the critical plasma density for 800-nm wavelength light and preferentially absorbs the ultrashort pulse for higher-efficiency plasma and EMP generation. We attempted to spectrally diagnose the plasma density and temperature using time-resolved spectroscopy of the laser-induced plasma as has been done previously.²⁴ However, time-gating our spectrometer with the necessary nanosecond-scale resolution resulted in signal levels that were too low for the intensified CCD in our spectrometer. We plan to directly measure the plasma density using optical interferometry²⁵ in the near future.

We believe that a previously published model²⁶ may explain our observation that 6-ns pump/probe delay results in the greatest EMP enhancement for both metal and dielectric targets. In Ref. 26, we find a one-dimensional

hydrodynamic model for simulation of nanosecond laser ablation of copper with peak pump laser intensity varied up to one half of that in our experiment (though the laser wavelength is 266 nm). At delays greater than 20 ns after the pulse is incident on the target, the simulated plasma density does not exceed the critical density for 266-nm wavelength light ($1.6 \times 10^{22} \text{ cm}^{-3}$). Pump laser pulses of increasing peak intensity were shown to couple less and less efficiently to the plasma, owing to the onset of plasma shielding earlier in time. In particular, for a 10-ns FWHM pulse with 10-GW/cm² peak intensity, the onset of plasma shielding occurs at 9 ns prior to the peak of the pulse. At that time, there is a sudden drop in laser intensity that reaches the target surface: from the maximum value to almost zero over just 1 ns. The quick drop-off of laser power is followed by a slightly less sudden increase and then a slower decrease. This result shows that there is a time window for extremely efficient blocking of 266-nm light at the target surface that is shorter than the time scale of the nanosecond laser pulse. Though the authors do not claim that the quick drop and rise in laser power at the target surface is due to resonant laser absorption, this may be the case. Summarily, for time scales shorter than the duration of the nanosecond pulse, the simulations result in an induced plasma density on copper that is very near to and sometimes above the critical density.

The authors of the work in Ref. 26 examined similar experimental parameters with a 1-atm Helium gas background²⁷ and found qualitatively similar results, albeit without the sharp, 1 to 2-ns scale laser reflection/absorption feature. We infer from this simulations that the nanosecond pulse-generated plasma density in our experiment can be near the critical density for absorption of the femtosecond laser wavelength, and that the plasma density may encourage efficient transmission and eventual absorption of the femtosecond laser pulse, when the femtosecond pulse is incident on the target sometime within the duration of the nanosecond laser pulse. We further extrapolate that more efficient absorption of the femtosecond laser pulse by the plasma resulted in more efficient conversion to EMP energy.

4 Conclusion

We have shown that EMP energy generated on glass and copper targets by a 38-fs laser pulse can be greatly enhanced by target surface plasma prepared on by a nanosecond laser pulse. We have shown several orders of magnitude enhancement for both copper and borosilicate glass targets.

The density profile of the preprepared plasma likely leads to the observed phenomena. Simulation and experimental determination of the plasma density will increase our understanding of the EMP enhancement effect.

Acknowledgments

The authors thank J. Penano and A. Ting for helpful discussions. This work was supported by the Joint Technology Office for High Energy Lasers, the Naval Research Laboratory, and the Johns Hopkins University Applied Physics Laboratory.

References

1. D. von der Linde, T. Engers, and G. Jenke, "Generation of high-order harmonics from solid surfaces by intense femtosecond laser pulses," *Phys. Rev. A* **52**, R25–R27 (1995).
2. Z. Chang et al., "Generation of coherent soft X rays at 2.7 nm using high harmonics," *Phys. Rev. Lett.* **79**(16), 2967–2970 (1997).
3. A. Rousse et al., "Efficient K α x-ray source from femtosecond laser-produced plasmas," *Phys. Rev. E* **50**(3), 2200–2207 (1994).
4. K. Wilson and V. Yakovlev, "Ultrafast rainbow: tunable ultrashort pulses from a solid-state kilohertz system," *J. Opt. Soc. Am. B* **14**(2), 444–448 (1997).
5. M. R. X. de Barros et al., "High-repetition-rate femtosecond mid-infrared pulse generation," *Opt. Lett.* **20**(5), 480–482 (1995).
6. A. Bonvalet et al., "Generation of ultrabroadband femtosecond pulses in the mid-infrared by optical rectification of 15 fs light pulses at 100 MHz repetition rate," *Appl. Phys. Lett.* **67**(20), 2907 (1995).
7. B. B. Hu et al., "Free-space radiation from electro-optic crystals," *Appl. Phys. Lett.* **56**(6), 506–508 (1990).
8. P. R. Smith, D. H. Auston, and M. C. Nuss, "Subpicosecond photoconducting dipole antennas," *IEEE J. Q. Electron.* **24**(2), 255–260 (1988).
9. S. Tzortzakis et al., "Coherent subterahertz radiation from femtosecond infrared filaments in air," *Opt. Lett.* **27**(21), 1944–1946 (2002).
10. K.-Y. Kim et al., "Terahertz emission from ultrafast ionizing air in symmetry-broken laser fields," *Opt. Express* **15**(8), 4577–4584 (2007).
11. J. S. Pearlman and G. H. Dahlbacka, "Emission of rf radiation from laser-produced plasmas," *J. Appl. Phys.* **49**(1), 457–459 (1978).
12. D. C. Eder et al., "Mitigation of electromagnetic pulse (EMP) effects from short-pulse lasers and fusion neutrons," Lawrence Livermore National Laboratory Report LLNL-TR-411183 (2009).
13. P. Sprangle et al., "Ultrashort laser pulses and electromagnetic pulse generation in air and on dielectric surfaces," *Phys. Rev. E* **69**(6), 066415 (2004).
14. J. A. Aspiotis et al., "Detection and analysis of RF emission generated by laser-matter interactions," *Proc. SPIE* **6219**, 621908 (2006).
15. J. Miragliotta et al., "Detection of microwave emission from solid targets ablated with an ultrashort pulsed laser," *Proc. SPIE* **8037**, 80370N (2011).
16. J. Miragliotta et al., "Enhancement of electromagnetic pulse emission from ultrashort laser pulse irradiated solid targets," *Proc. SPIE* **8381**, 83811N (2012).
17. A. Couairon and A. Mysyrowicz, "Femtosecond filamentation in transparent media," *Phys. Rep.* **441**(2), 47–189 (2007).
18. M. Mlejnek, E. M. Wright, and J. V. Moloney, "Dynamic spatial replenishment of femtosecond pulses propagating in air," *Opt. Lett.* **23**(5), 382–384 (1998).
19. A. Couairon et al., "Infrared femtosecond light filaments in air: simulations and experiments," *J. Opt. Soc. Am. B* **19**(5), 1117–1131 (2002).
20. L. Berge et al., "Multiple filamentation of terawatt laser pulses in air," *Phys. Rev. Lett.* **92**(22), 225002 (2004).
21. M. Kolesik and J. V. Moloney, "Modeling and simulation techniques in extreme nonlinear optics of gaseous and condensed media," *Rep. Progr. Phys.* **77**(1), 016401 (2014).
22. W. Li and D. Y. Li, "On the correlation between surface roughness and work function in copper," *J. Chem. Phys.* **122**(6), 064708 (2005).
23. M. Lenzen et al., "Femtosecond optical breakdown in dielectrics," *Phys. Rev. Lett.* **80**(18), 4076–4079 (1998).
24. J. R. Freeman et al., "Comparison of optical emission from nanosecond and femtosecond laser produced plasma in atmosphere and vacuum conditions," *Spectrochim. Acta Part B: Atom. Spectrosc.* **87**, 43–50 (2013).
25. Y.-H. Chen et al., "Direct measurement of the electron density of extended femtosecond laser pulse-induced filaments," *Phys. Rev. Lett.* **105**(21), 215005 (2010).
26. A. Bogaerts et al., "Laser ablation for analytical sampling: what can we learn from modeling?," *Spectrochim. Acta Part B: Atom. Spectrosc.* **58**(11), 1867–1893 (2003).
27. Z. Chen and A. Bogaerts, "Laser ablation of Cu and plume expansion into 1 atm ambient gas," *J. Appl. Phys.* **97**(6), 063305 (2005).

Sanjay Varma is a senior staff member of the Johns Hopkins University Applied Physics Laboratory. He earned his BS in electrical engineering from Princeton University in 2003 and his PhD in electrical engineering from the University of Maryland, College Park in 2011. He currently researches nonlinear optics with high intensity femtosecond laser pulses for research in plasma physics and biophysics.

Jane Spicer is a principal staff member of the Johns Hopkins University Applied Physics Laboratory. She earned her BSc and MSc degrees in physics and metallurgical engineering from Queen's University in 1979 and 1983, respectively, and her PhD in materials engineering from Johns Hopkins University in 1986. She has expertise in optics, materials science and nondestructive evaluation. She currently conducts research and development of metamaterial structures for radar tagging and standoff methods for explosives detection.

Benjamin Brawley is a senior staff member of the Johns Hopkins University Applied Physics Laboratory. He earned his BS in electrical engineering from Penn State University in 2001 and his MS in electrical and computer engineering from Johns Hopkins University in 2006. He is a radio frequency and antenna design engineer with extensive background in hardware development, propagation analysis, and system level performance testing.

Joseph Miragliotta is a principal staff member of the Johns Hopkins University Applied Physics Laboratory. He received his MS and PhD degrees in physics from Rensselaer Polytechnic Institute in 1985 and 1987, respectively. In addition to his work with ultrashort pulsed lasers, his current research includes the development of microwave and IR metamaterials for the low-profile antennas, absorbers, and filters for applications that include nonmechanical beam steering, and chemical/biological sensing.